# ELECTRONIC SUPPLEMENTARY INFORMATION

Exploring the coordination capabilities of a family of flexible benzotriazole-based ligands using Cobalt (II) sources

Edward Loukopoulos,[a] Nicholas F. Chilton,[b] Alaa Abdul-Sada,[a] and George E. Kostakis*[a]

[a] Department of Chemistry, School of Life Sciences, University of Sussex, Brighton BN1 9QJ, United Kingdom. E-mail: G.Kostakis@sussex.ac.uk

[b] School of Chemistry, The University of Manchester, Manchester M13 9PL, United Kingdom

| Table of contents | Page |
|---|---|

| **Figure S12-S14.** TGA graphs and analysis for compounds **1**, **5**, **7**. | S13-S14 |
|---|---|

**Table S1.** Crystal data and structure refinement for **1**-**5**.

| Compound | **1**·2MeCN | **2** | **3**·MeCN | **4** | **5**·2MeCN |
|---|---|---|---|---|---|
| Empirical formula | $C_{44}H_{38}Cl_4Co_2N_{14}$ | $C_{40}H_{32}Br_4Co_2N_{12}$ | $C_{22}H_{19}Cl_2CoN_7$ | $C_{20}H_{16}Cl_2CoN_6$ | $C_{44}H_{38}Br_4Co_2N_{14}$ |
| Formula weight | 1022.54 | 1118.27 | 511.27 | 470.22 | 1200.38 |
| Temperature/K | 173.0 | 293(2) | 173.0 | 173 | 173.0 |
| Crystal system | triclinic | triclinic | triclinic | monoclinic | triclinic |
| Space group | P-1 | P-1 | P-1 | $P2_1/c$ | P-1 |
| a/Å | 9.2872(6) | 9.4548(5) | 10.3450(9) | 10.1342(8) | 10.4914(10) |
| b/Å | 11.0385(9) | 10.7016(8) | 10.6249(10) | 21.3347(15) | 10.8202(10) |
| c/Å | 13.0562(8) | 10.7793(9) | 12.4219(11) | 9.7278(11) | 12.3408(11) |
| α/° | 67.511(7) | 68.392(7) | 79.192(7) | 90 | 79.793(8) |
| β/° | 84.255(5) | 81.206(6) | 72.669(8) | 109.334(10) | 73.864(8) |
| γ/° | 79.656(6) | 83.475(5) | 72.588(8) | 90 | 72.821(9) |
| Volume/Å$^3$ | 1215.87(15) | 1000.14(13) | 1236.4(2) | 1984.7(3) | 1278.8(2) |
| Z | 1 | 1 | 2 | 4 | 1 |
| $\rho_{calc}$g/cm$^3$ | 1.397 | 1.857 | 1.373 | 1.574 | 1.559 |
| μ/mm$^1$ | 7.744 | 4.873 | 0.933 | 1.154 | 3.818 |
| F(000) | 522.0 | 550.0 | 522.0 | 956.0 | 594.0 |
| Crystal size/mm$^3$ | 0.08 × 0.06 × 0.03 | 0.093 × 0.055 × 0.031 | 0.28 × 0.2 × 0.18 | 0.38 × 0.29 × 0.25 | 0.26 × 0.2 × 0.1 |
| Radiation | CuKα (λ = 1.54184) | MoKα (λ = 0.71073) | MoKα (λ = 0.71073) | MoKα (λ = 0.71073) | Mo Kα (λ = 0.71073) |
| 2Θ range for data collection/° | 8.774 to 142.54 | 5.616 to 52.744 | 6.912 to 58.188 | 7.14 to 59.038 | 7.604 to 52.742 |
| Index ranges | -9 ≤ h ≤ 11, -13 ≤ k ≤ 13, -11 ≤ l ≤ 16 | -11 ≤ h ≤ 10, -13 ≤ k ≤ 13, -13 ≤ l ≤ 13 | -12 ≤ h ≤ 13, -13 ≤ k ≤ 9, -16 ≤ l ≤ 16 | -12 ≤ h ≤ 12, -27 ≤ k ≤ 27, -13 ≤ l ≤ 12 | -13 ≤ h ≤ 12, -13 ≤ k ≤ 14, -7 ≤ l ≤ 16 |
| Reflections collected | 4518 | 11760 | 8046 | 8647 | 5739 |
| Independent reflections | 4518 [$R_{int}$ = 0.0571, $R_{sigma}$ = 0.0893] | 4014 [$R_{int}$ = 0.1146, $R_{sigma}$ = 0.0833] | 5498 [$R_{int}$ = 0.0248, $R_{sigma}$ = 0.0516] | 4428 [$R_{int}$ = 0.0812, $R_{sigma}$ = 0.1051] | 3973 [$R_{int}$ = 0.0222, $R_{sigma}$ = 0.0514] |
| Data/restraints/parameters | 4518/1/290 | 4014/0/262 | 5498/24/290 | 4428/0/262 | 3973/13/290 |
| Goodness-of-fit on F$^2$ | 1.019 | 1.385 | 1.012 | 1.013 | 1.026 |
| Final R indexes [I>=2σ (I)] | $R_1$ = 0.0717, $wR_2$ = 0.1813 | $R_1$ = 0.0719, $wR_2$ = 0.1873 | $R_1$ = 0.0385, $wR_2$ = 0.0888 | $R_1$ = 0.0753, $wR_2$ = 0.1787 | $R_1$ = 0.0424, $wR_2$ = 0.1019 |
| Final R indexes [all data] | $R_1$ = 0.0895, $wR_2$ = 0.2011 | $R_1$ = 0.0938, $wR_2$ = 0.1995 | $R_1$ = 0.0495, $wR_2$ = 0.0954 | $R_1$ = 0.1242, $wR_2$ = 0.2174 | $R_1$ = 0.0562, $wR_2$ = 0.1100 |
| Largest diff. peak/hole / e Å$^{-3}$ | 1.26/-0.52 | 1.67/-0.82 | 0.43/-0.48 | 1.08/-1.31 | 0.53/-0.41 |

**Table S2.** Crystal data and structure refinement for **6-10**.

| Compound | **6**·2MeCN | **7**·2MeCN | **8** | **9** | **10** |
|---|---|---|---|---|---|
| Empirical formula | $C_{44}H_{38}CoN_{16}O_6$ | $C_{22}H_{19}Cl_2CoN_7$ | $C_{40}H_{32}Cl_4Co_2N_{12}$ | $C_{40}H_{32}N_{12}Co_2Br_4$ | $C_{40}H_{32}CoN_{14}O_6$ |
| Formula weight | 945.83 | 511.27 | 940.43 | 1118.27 | 863.72 |
| Temperature/K | 173.0 | 173 | 173.0 | 173.0 | 173.0 |
| Crystal system | monoclinic | monoclinic | triclinic | triclinic | triclinic |
| Space group | $P2_1/c$ | $P2_1/c$ | | | |
| a/Å | 10.3683(6) | 12.7902(11) | 10.0907(18) | 10.1947(9) | 9.8734(7) |
| b/Å | 24.1547(10) | 8.7966(8) | 10.4778(13) | 10.5735(11) | 10.0969(7) |
| c/Å | 9.1109(4) | 20.363(2) | 11.011(2) | 11.0714(12) | 10.6672(9) |
| α/° | 90 | 90 | 83.817(13) | 81.303(9) | 96.504(6) |
| β/° | 110.136(6) | 100.365(10) | 77.419(16) | 77.374(8) | 112.290(7) |
| γ/° | 90 | 90 | 63.231(16) | 62.179(10) | 99.774(6) |
| Volume/$Å^3$ | 2142.29(19) | 2253.6(4) | 1014.4(3) | 1028.3(2) | 951.10(13) |
| Z | 2 | 4 | 1 | 1 | 1 |
| $\rho_{calc}g/cm^3$ | 1.466 | 1.507 | 1.540 | 1.806 | 1.508 |
| $\mu/mm^1$ | 3.732 | 1.024 | 1.129 | 4.739 | 4.128 |
| F(000) | 978.0 | 1044.0 | 478.0 | 550.0 | 445.0 |
| Crystal size/$mm^3$ | 0.2 × 0.1 × 0.08 | 0.12 × 0.09 × 0.06 | 0.12 × 0.08 × 0.04 | 0.36 × 0.24 × 0.18 | 0.4 × 0.28 × 0.14 |
| Radiation | CuKα (λ = 1.54184) | MoKα (λ = 0.71073) | MoKα (λ = 0.71073) | MoKα (λ = 0.71073) | CuKα (λ = 1.54184) |
| 2Θ range for data collection/° | 10.972 to 140.372 | 7.296 to 57.968 | 7.584 to 58.59 | 7.556 to 58.686 | 9.062 to 142.056 |
| Index ranges | $-7 \le h \le 12$, $-25 \le k \le 29$, $-11 \le l \le 10$ | $-17 \le h \le 17$, $-7 \le k \le 11$, $-26 \le l \le 15$ | $-12 \le h \le 13$, $-9 \le k \le 14$, $-11 \le l \le 14$ | $-13 \le h \le 13$, $-13 \le k \le 12$, $-15 \le l \le 15$ | $-8 \le h \le 12$, $-12 \le k \le 12$, $-13 \le l \le 13$ |
| Reflections collected | 6575 | 8556 | 6761 | 7075 | 5125 |
| Independent reflections | 3936 [$R_{int}$ = 0.0254, $R_{sigma}$ = 0.0421] | 5048 [$R_{int}$ = 0.0326, $R_{sigma}$ = 0.0548] | 4567 [$R_{int}$ = 0.0436, $R_{sigma}$ = 0.1116] | 4605 [$R_{int}$ = 0.0352, $R_{sigma}$ = 0.0697] | 3503 [$R_{int}$ = 0.0455, $R_{sigma}$ = 0.0624] |
| Data/restraints/parameters | 3936/0/305 | 5048/0/290 | 4567/0/262 | 4605/0/262 | 3503/0/277 |
| Goodness-of-fit on $F^2$ | 1.030 | 1.040 | 1.033 | 1.007 | 1.043 |
| Final R indexes [I>=2σ (I)] | $R_1$ = 0.0389, $wR_2$ = 0.0960 | $R_1$ = 0.0478, $wR_2$ = 0.0996 | $R_1$ = 0.0611, $wR_2$ = 0.1014 | $R_1$ = 0.0427, $wR_2$ = 0.0813 | $R_1$ = 0.0584, $wR_2$ = 0.1562 |
| Final R indexes [all data] | $R_1$ = 0.0473, $wR_2$ = 0.1014 | $R_1$ = 0.0742, $wR_2$ = 0.1175 | $R_1$ = 0.1082, $wR_2$ = 0.1274 | $R_1$ = 0.0625, $wR_2$ = 0.0904 | $R_1$ = 0.0643, $wR_2$ = 0.1677 |
| Largest diff. peak/hole / e $Å^{-3}$ | 0.42/-0.32 | 0.33/-0.36 | 0.58/-0.52 | 0.69/-0.84 | 0.43/-0.70 |

**Table S3.** π–π stacking distances (Å) and angles (º) in compound **1**.

| Rings | Distance between ring centroids (Å) | Perpendicular distance between ring planes (Å) | Centroid offset (Å) | Dihedral angle between ring mean-planes (˚) |
|---|---|---|---|---|
| A-A$^{i}$ | 3.708(3) | 3.433(2) | 1.400(2) | 0.0 |
| A-B$^{i}$ | 3.596(3) | 3.436(2) | 1.400(2) | 0.8(3) |
| C-C$^{ii}$ | 3.755(3) | 3.472(2) | 1.430(2) | 0.0 |

Rings: A: C15-C16-N4-N5-N6. B: C15-C16-C17-C18-C19-C20. C: C2-C3-C4-C5-C6-C7.

Symmetry codes: $^{i}$: 2-x, -y, 1-z. $^{ii}$: 1-x, 1-y, 2-z.

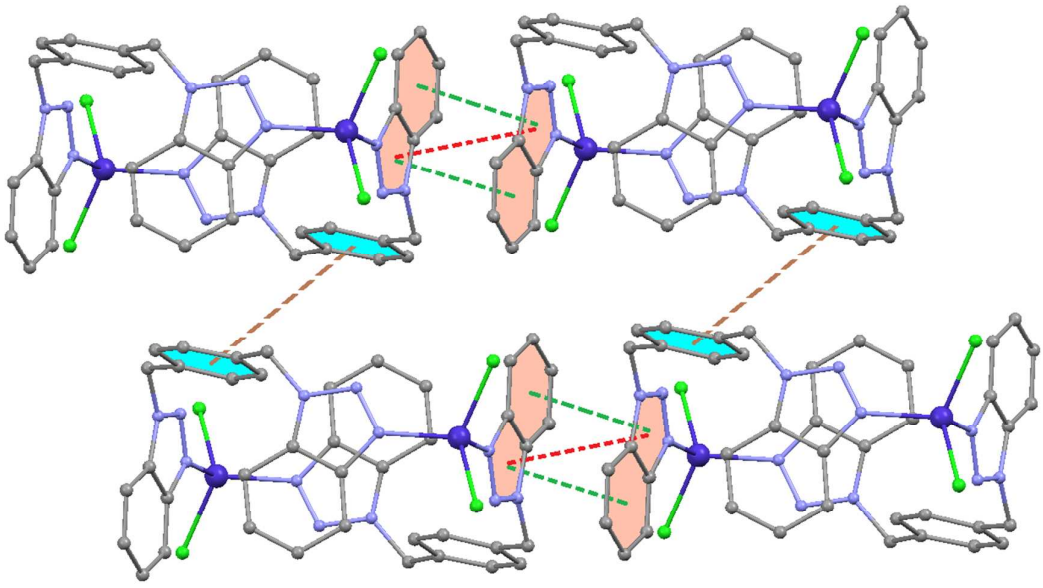

**Figure S1.** Part of the supramolecular architecture of compound **1**, stabilised by intermolecular π···π interactions (brown, green and red dashed lines), as described in Table

S3. Solvent molecules and hydrogen atoms have been omitted. Color code Co (blue), Cl (green), C (grey), N (light blue).

**Table S4.** π–π stacking distances (Å) and angles (º) in compound **3**.

| Rings | Distance between ring centroids (Å) | Perpendicular distance between ring planes (Å) | Centroid offset (Å) | Dihedral angle between ring mean-planes (˚) |
|---|---|---|---|---|
| A-A$^{i}$ | 3.6485(13) | 3.3288(9) | 1.413(8) | 0.00 (13) |
| A-B$^{i}$ | 3.4601(13) | 3.3291 (9) | 0.938(8) | 0.08(12) |

Rings: A: C1-C6-N1-N2-N3. B: C1-C2-C3-C4-C5-C6.

Symmetry codes: $^{i}$: 2-x, 1-y, 1-z.

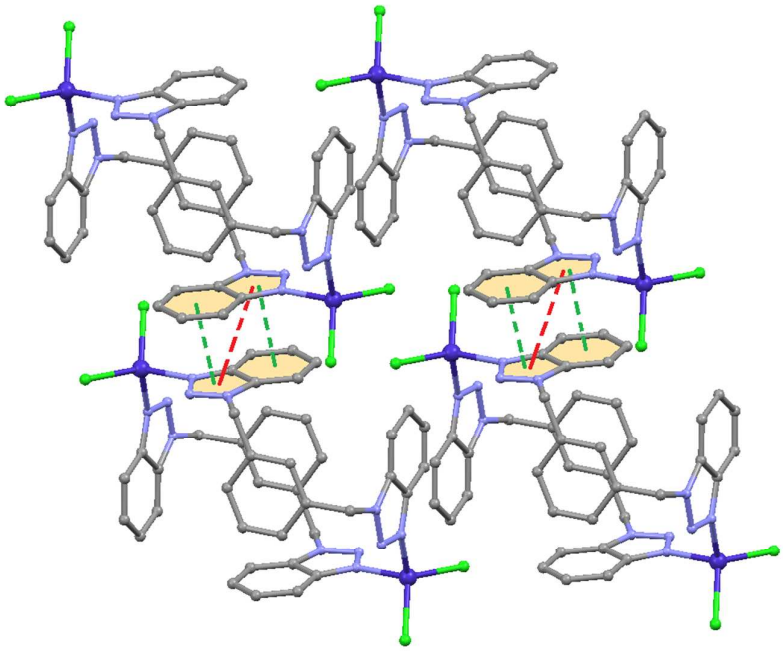

**Figure S2.** Part of the supramolecular architecture of compound **3**, stabilised by intermolecular π···π interactions (green and red dashed lines), as described in Table S4.

Solvent molecules and hydrogen atoms have been omitted. Color code Co (blue), Cl (green), C (grey), N (light blue).

**Table S5.** π–π stacking distances (Å) and angles (º) in compound **4**.

| Rings | Distance between ring centroids (Å) | Perpendicular distance between ring planes (Å) | Centroid offset (Å) | Dihedral angle between ring mean-planes (˚) |
|---|---|---|---|---|
| A-A$^{i}$ | 3.641(3) | 3.2927(17) | 1.554(2) | 0.0(2) |
| A-B$^{i}$ | 3.801(3) | 3.3155(17) | 1.902(2) | 0.8(2) |

Rings: A: C1-C2-C3-C4-C5-C6. B: C1-C6-N1-N2-N3.

Symmetry codes: $^{i}$: -x, 1-y, -z.

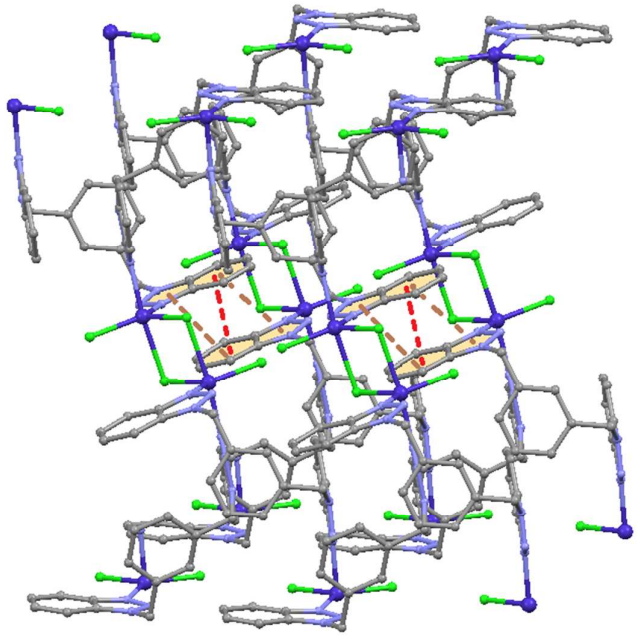

**Figure S3.** Part of the supramolecular architecture of compound **4**, in which the intermolecular π···π interactions (described in Table S5, noted with brown and red dashed

lines), further stabilise the 2D framework. Hydrogen atoms have been omitted. Color code Co (blue), Cl (green), C (grey), N (light blue).

**Table S6.** π–π stacking distances (Å) and angles (º) in compound **8**.

| Rings | Distance between ring centroids (Å) | Perpendicular distance between ring planes (Å) | Centroid offset (Å) | Dihedral angle between ring mean-planes (˚) |
|---|---|---|---|---|
| A-B$^{i}$ | 3.782(3) | 3.3773(17) | 1.661(3) | 0.9(2) |
| C-C$^{ii}$ | 3.688(3) | 3.2972(18) | 1.651(3) | 0.0(2) |

Rings: A: C1-C6-N1-N2-N3. B: C1-C2-C3-C4-C5-C6. C: C15-C16-C17-C18-C19-C20.

Symmetry codes: $^{i}$: -x, 1-y, 1-z. $^{ii}$: 1-x, -y, 2-z.

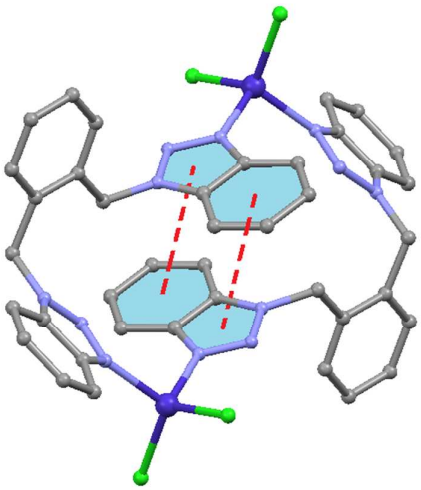

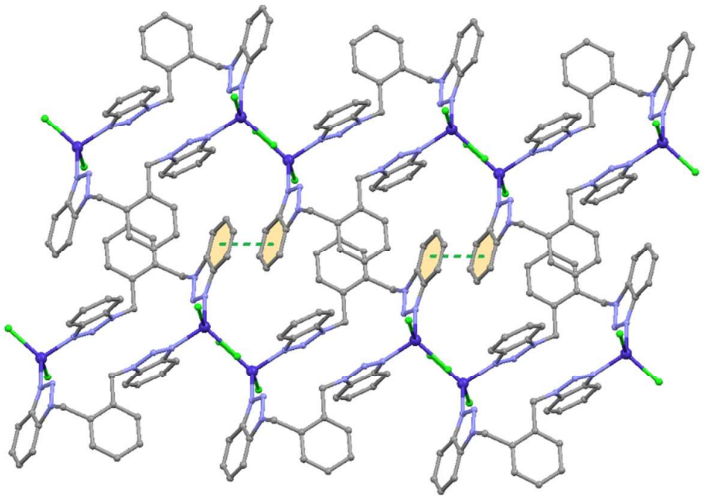

**Figure S4.** (upper) The intramolecular π···π interactions observed in compound **8**, noted with red dashed lines. (lower) Part of the supramolecular architecture of the compound **8**, stabilised by the intermolecular π···π interactions (noted with green dashed lines). Hydrogen atoms have been omitted. Color code Co (blue), Cl (green), C (grey), N (light blue).

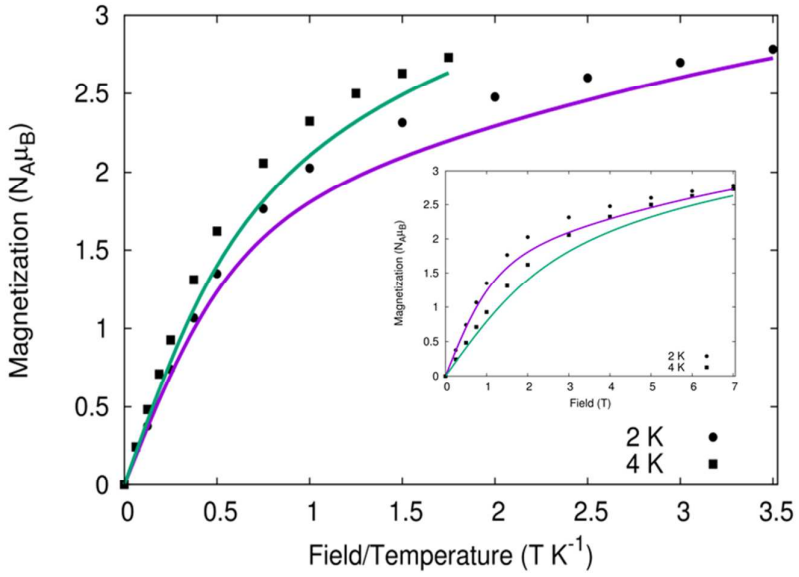


**Figure S5.** Experimental (black circles and squares) and fitted (purple and green lines, parameters in text) reduced magnetization for **7** at 2 and 4 K. (inset) Experimental (black

circles and squares) and fitted (purple and green lines, parameters in text) magnetization for **7** at 2 and 4 K.

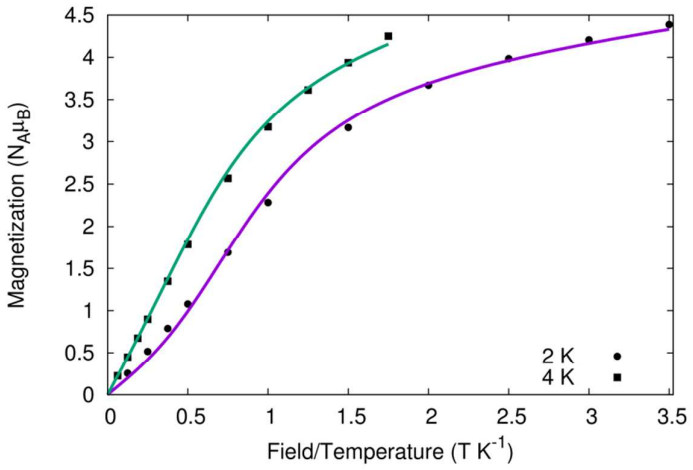


**Figure S6.** Experimental (black circles and squares) and fitted (purple and green lines) reduced magnetization for **9** at 2 and 4 K.

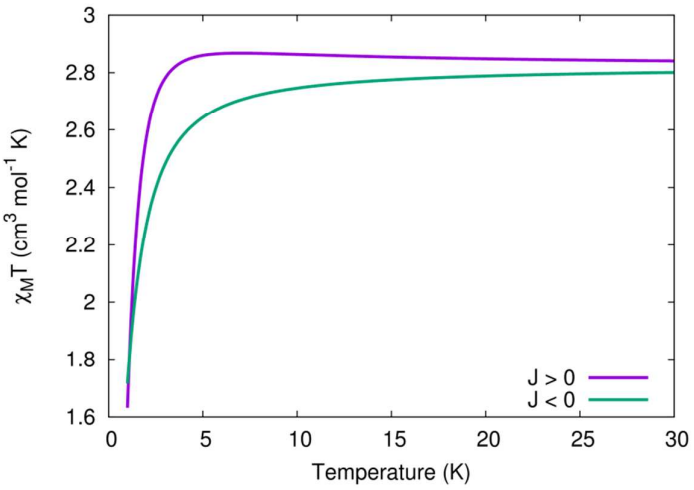


**Figure S7.** Simulated $\chi_M T$ in an 0.5 T field for $J > 0$ and $J < 0$ using the $S = 1/2$ model used to simulate the EPR spectra of compound **4**.

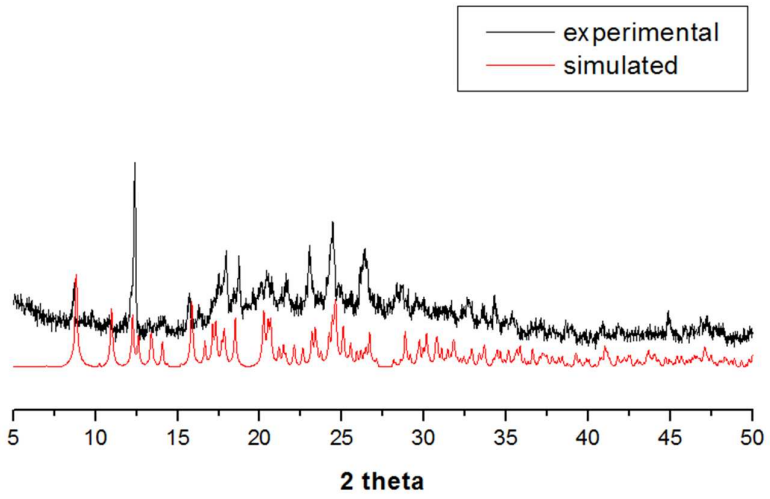


**Figure S8**. The powder XRD pattern of compound **7** (experimental and simulated from the crystal structure).

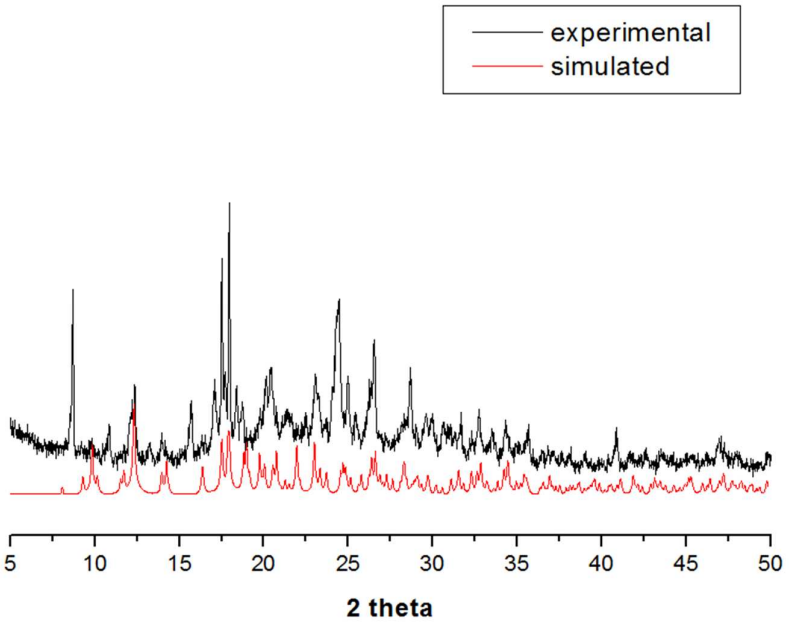


**Figure S9**. The powder XRD pattern of compound **8** (experimental and simulated from the crystal structure).

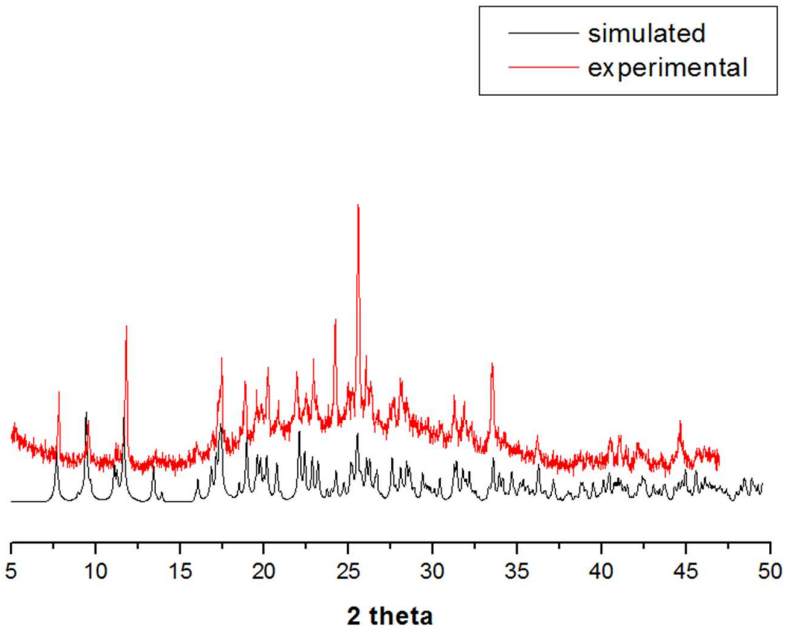


**Figure S10**. The powder XRD pattern of compound **9** (experimental and simulated from the crystal structure).

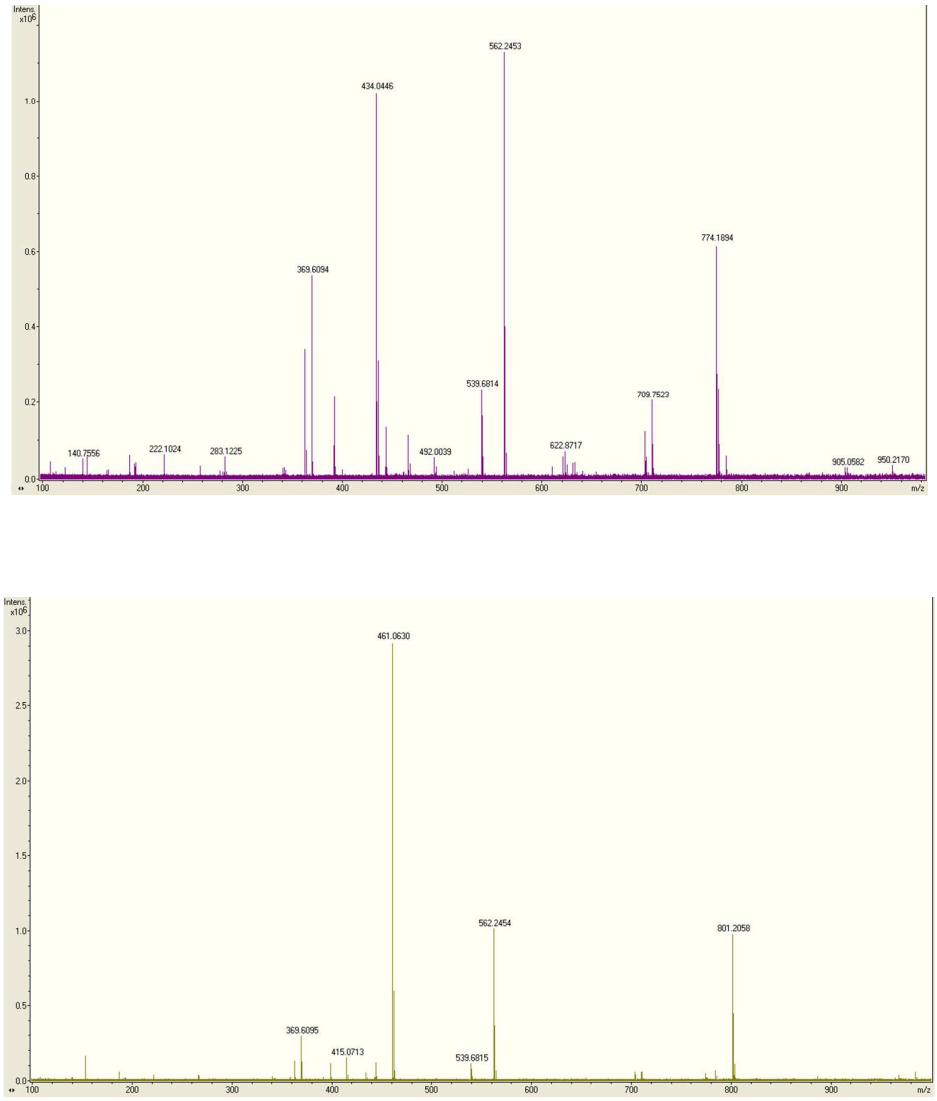


**Figure S11.** Representative ESI-MS graphs for compounds **4** (upper) and **10** (lower).

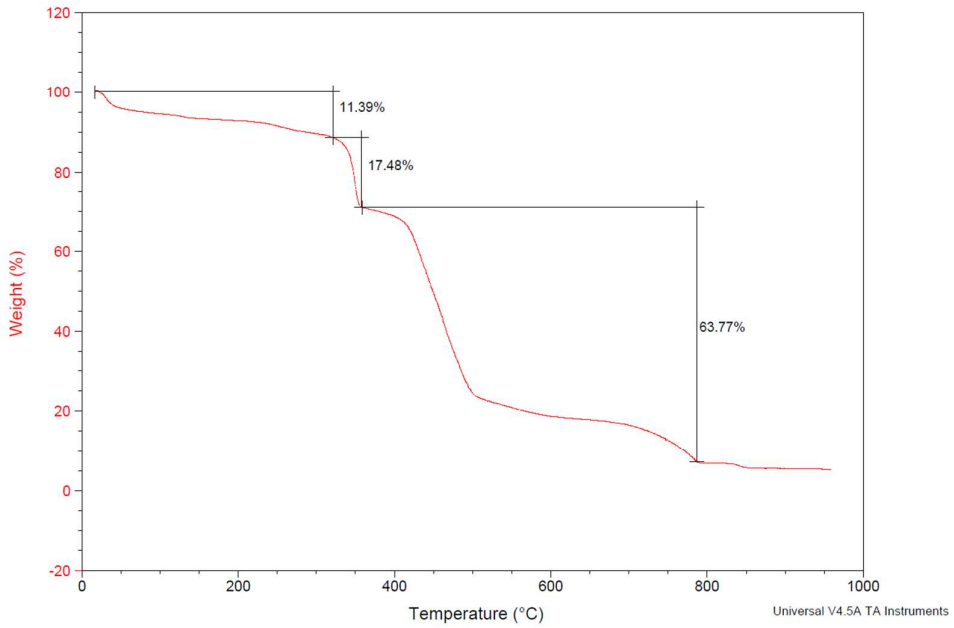


**Figure S12.** TGA graph for compound **1**. 1st mass loss: 9.02% calc. for two MeCN solvents. 2nd mass loss: 13.87% for four Cl atoms. 3rd mass loss: 63.45% calc. for framework decomposition.

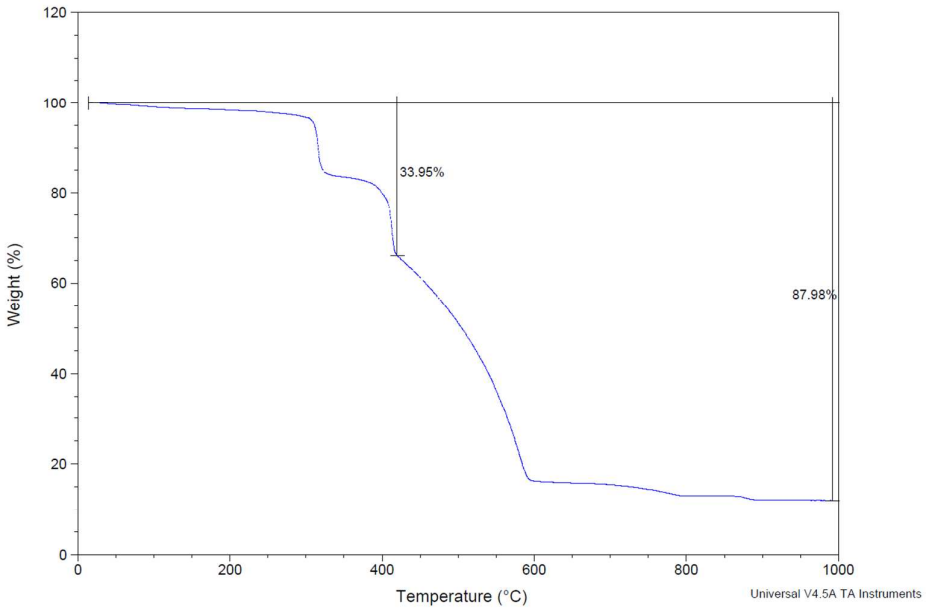


**Figure S13.** TGA graph for compound **5**. 1st mass loss: 33.47% calc. for two MeCN solvents and four Br atoms. 2nd mass loss: 54.03% obs., 54.04% calc. for framework decomposition.

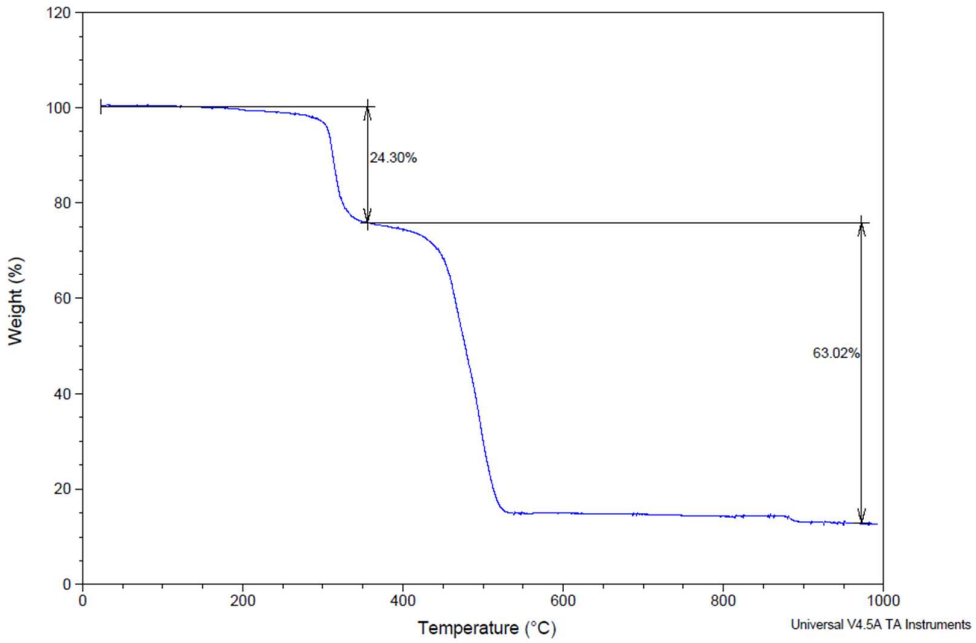


**Figure S14.** TGA graph for compound **7**. 1st mass loss: 22.09% calc. for one MeCN solvent and two Cl atoms. 2nd mass loss: 63.25% calc. for framework decomposition.